Kinetic Modeling of Fatty Acid Methyl Esters and Triglycerides Hydrodeoxygenation over Nickel and Palladium Catalysts

Imane Hachemi, Dmitry Yu. Murzin

PII: S1385-8947(17)32075-2
DOI: https://doi.org/10.1016/j.cej.2017.11.153
Reference: CEJ 18124

To appear in: *Chemical Engineering Journal*

Received Date: 7 August 2017
Revised Date: 20 November 2017
Accepted Date: 23 November 2017

Please cite this article as: I. Hachemi, D.Y. Murzin, Kinetic Modeling of Fatty Acid Methyl Esters and Triglycerides Hydrodeoxygenation over Nickel and Palladium Catalysts, *Chemical Engineering Journal* (2017), doi: https://doi.org/10.1016/j.cej.2017.11.153

Kinetic Modeling of Fatty Acid Methyl Esters and Triglycerides Hydrodeoxygenation over Nickel and Palladium Catalysts

Imane Hachemi, Dmitry Yu. Murzin*

Laboratory of Industrial Chemistry and Reaction Engineering,

Åbo Akademi University, Åbo/Turku, Finland

*dmurzin@abo.fi

Abstract

The kinetics of fatty acids methyl esters (FAME) and triglycerides (TG) hydrodeoxygenation (HDO) over 5 wt % Ni/H-Y-80 and 5 wt % Pd/C catalysts into green-diesel range hydrocarbons was studied experimentally and modeled numerically. The liquid-phase HDO was performed in a semi-batch reactor at the reaction temperature of 300 °C and pressure 30 bar on a sulfur free nickel supported catalyst and a palladium catalyst for comparison.

The fit of the model was evaluated by comparing the concentration profiles obtained from the model with the experimental data. The model confirmed that a complete reaction network involves hydrogenation, decarboxylation/decarbonylation and the direct hydrodeoxygenation of FA. Overall, the model displayed a good fitting for both studied substrates. Moreover, the model is expected to be applicable to different fatty acids. The rate constants for the conversion of FAME and TG, containing mixture of two groups of molecules C:16 and C:18, show dependence on the fatty acids carbon chain length.

1. Introduction

Over the recent decade, considerable efforts have been made to develop clean and renewable fuels technologies in order to secure the world energy reserves and gain environment benefits. The green- house gases emissions increase was partly reduced by a continuing decline in the emissions from the road transportation through the use of renewable energy. At the end of 2011, almost all European countries were on a track towards their Kyoto protocol targets for 2008–2012 [1]. Research on the fuel production from biomass has been motivated by a desire to displace fossil fuels and to mitigate CO_2 emissions and the associated global warming. Biofuels are more sustainable and cleaner energy carriers than fossil fuels reducing emissions of CO_2 and of S- and N-containing pollutants. Thus, they remain the most attractive alternative renewable fuels.

The conversion of the fatty acids (FA) into diesel range hydrocarbons compatible with petroleum diesel, which is coined renewable diesel, has been studied using hydrodeoxygenation. Various catalysts were investigated including sulfided NiMo and CoMo catalysts [2], noble metal catalysts such as Pd and Pt [3,4], and sulfur free Ni based catalysts. Over the last decade many studies revealed promising results in the utilization of sulfur free supported Ni catalysts [5–8].

Literature studies [9–11] report that HDO process starts with saturation of the double bonds C=C present in the alkyl chain followed by the cleavage of C–O bond forming a fatty acid. This later undergoes further hydrogenation forming an aldehyde which is rapidly transformed into the corresponding alcohol. Aliphatic hydrocarbons are produced via three different routes namely decarboxylation of fatty acids, decarbonylation of aldehydes and deoxygenation of alcohols. In view of the foregoing,

non-precious metal catalysts comprising supports other than carbon – particularly Ni on oxidic supports and hydrotalcite materials showed high performance in fatty acids deoxygenation. The occurrence of hydrodeoxygenation (HDO) or decarboxylation/decarbonylation (DCO_x) is highly dependent on the catalyst used. HDO of fatty acids (FA) has been investigated over a large range of different catalysts [10,12,13]. It has been shown that deoxygenation (DO) over Pd and Pt tends to occur via DCO resulting in high yields of C_{n-1} hydrocarbons [14–16]. Ni supported catalysts demonstrated production alkanes via HDO and DCO_x. Moreover, the selectivity depends on the supports acidity [10,16–20].

In the previous work of the authors [16] FA HDO was investigated in depth using fatty acids methyl esters (FAME) extracted from chlorella alga [21], tall oil fatty acids (TOFA) and animal fat triglyceride [22] (TG). FA's were introduced in a semi-batch reactor at the reaction temperature of 300 °C and pressure 30 bar. The reactions were performed in the inert solvent dodecane with a stirring rate corresponding to 1200 rpm. Ni sulfur-free supported catalysts were used in that study, which was mainly qualitative without any quantification of kinetic dependencies. For comparison purposes a commercial Pd/C catalysts was also evaluated in [16].

Knowledge of the kinetics is, however, important not only for the reactor design, but also for understanding of the reaction mechanisms. Therefore, the goal of this work was to perform kinetic modelling for HDO of FAME and TG over 5 wt% Ni supported on H-Y-80 where aliphatic hydrocarbons are formed. Information about the catalyst, characterization data and procedure of catalytic experiments was reported in detail in [16]. For comparative purposes also kinetic modelling of the same feedstock over a commercial Pd/C catalyst was done. Kinetics of other fatty acids deoxygenation

reactions has been investigated previously [18,23–25] over different catalysts using several model molecules.

In this work, kinetic modelling of hydrodeoxygenation of the real substrates, such as animal fat (TG) and *Chlorella alga* biodiesel (FAME) over Ni and Pd catalysts, was performed.

It should be also noted that in the current paper, the kinetic data are presented in a more detailed way than in the original work [16] reporting for instance the concentration profiles of each compound in the mixture, whereas, in ref. 16, dedicated to catalyst synthesis characterization and testing, being thus devoid of any modelling, kinetic data were shown for lumped groups of reactants, intermediates and products.

A representative model was established based on a typical reaction network.

2. Experimental section

While the experimental data has been reported previously the pertinent details are presented here to facilitate evaluation of catalytic results. The aim of the experiments was to acquire data to access and understand the reaction mechanism in order to develop a model taking into account the different steps of the reaction.

2.1. Materials

5 wt% Ni/H-Y-80 catalyst was synthesized by wetness impregnation evaporation method. Thereafter, the catalyst was dried and calcined in air at 400 °C for 4 hours followed by sieving [16, 26]. 5 wt% Pd/C was purchased from Sigma-Aldrich.

Fatty acids methyl esters (FAME) were obtained from Chlorella microalga (Fuqing King, Drarmsa Spirulina Co, Ltd, China) by in situ-transesterification which was performed at 60 °C for 4 hours in 20 wt% H_2SO_4 followed by purification with a clay

(Argila verde, www.forcadaterra.com, Brazil) [21]. FAME is composed mainly of saturated and unsaturated esters containing 25% methyl linoleate, 26% methyl linoleate, 32% methyl palmitate and 8% methyl palmitoleate.

Animal fat was provided by a refinery containing mainly C18 (17% C18:0, 43.4% C18:1) and C16 (24.1% C16:0, 3.1% C16:1) and longer fatty acids. SEC analysis showed that the animal fat contains 93.57 % triglycerides, 5.21 % diglycerides and 1.43 % monoglycerides [27].

2.2. Experimental procedure and analysis

Hydrodeoxygenation of fatty acids was carried in a semi-batch reactor at 300°C under 30 bar H_2. The reaction was run in a 300 ml stirred reactor equipped with a heating jacket. In all experiments 0.25 g of the catalyst was charged into the reactor with dodecane (Sigma Aldrich, ≥90%). The reactor was flushed with argon to remove oxygen. 1g/L of reactant was injected in a pre-reactor and bubbled with argon before being put into the reactor. Hydrodeoxygenation started when the substrate was introduced into the reactor at the desired temperature and pressure. The stirring rate corresponded to 1200 rpm. Prior to the run, the catalyst underwent a reduction step at the reduction temperature determined by TPR of supported nickel and palladium catalysts. The reduction was carried for 2 hours. Liquid samples taken from the reactor were silylated before analysis by gas chromatography (GC). The silylated samples were kept in an oven at 70°C for an hour before being injected in the GC equipped with a split column (film thickness 0.25 µm) under He pressure 1 bar flowing at 75 ml/min. The column was heated up to 300 °C and the signal was recorded with FID detector.

The triglycerides fraction was analyzed with the following procedure: 2 ml of MTBE containing the internal standards (0.04 mg each) was added to the samples. The internal

standards used are: (21:0) heneicosanoic acid (Sigma 99 %), betulinol (purified in our lab), cholesteryl heptadecanoate (Sigma > 95%) and 1,3-dipalmitoyl-2-oleoylglycerol (Sigma 99%). MTBE was evaporated under nitrogen stream at 40°C until only docosanol remained. The evaporation was repeated after 1 ml of acetone was added. 150 µl of the silylating reagent mixture (pyridine-BSTFA-TMCS 1:4:1) was added and then the final mixture was put for 45 minutes in 70°C oven. The silylated sample was injected in a gas chromatograph PerkinElmer Clarus 680, equipped with a FID detector and Agilent J&W HP-1/SIMDIST column (film thickness 0.15 µm) using H_2 (7 ml/min) as carrier gas. The column was heated up to 340 °C.

3. Kinetic modeling and data fitting

As discussed previously [16] the influence of mass transfer could be neglected due to vigorous stirring and application of small catalysts particles (< 63 µm). Scheme 1 represents the reaction network for FAME and TG HDO, showing the main reactions: hydrogenation, decarboxylation/decarbonylation and dehydration.

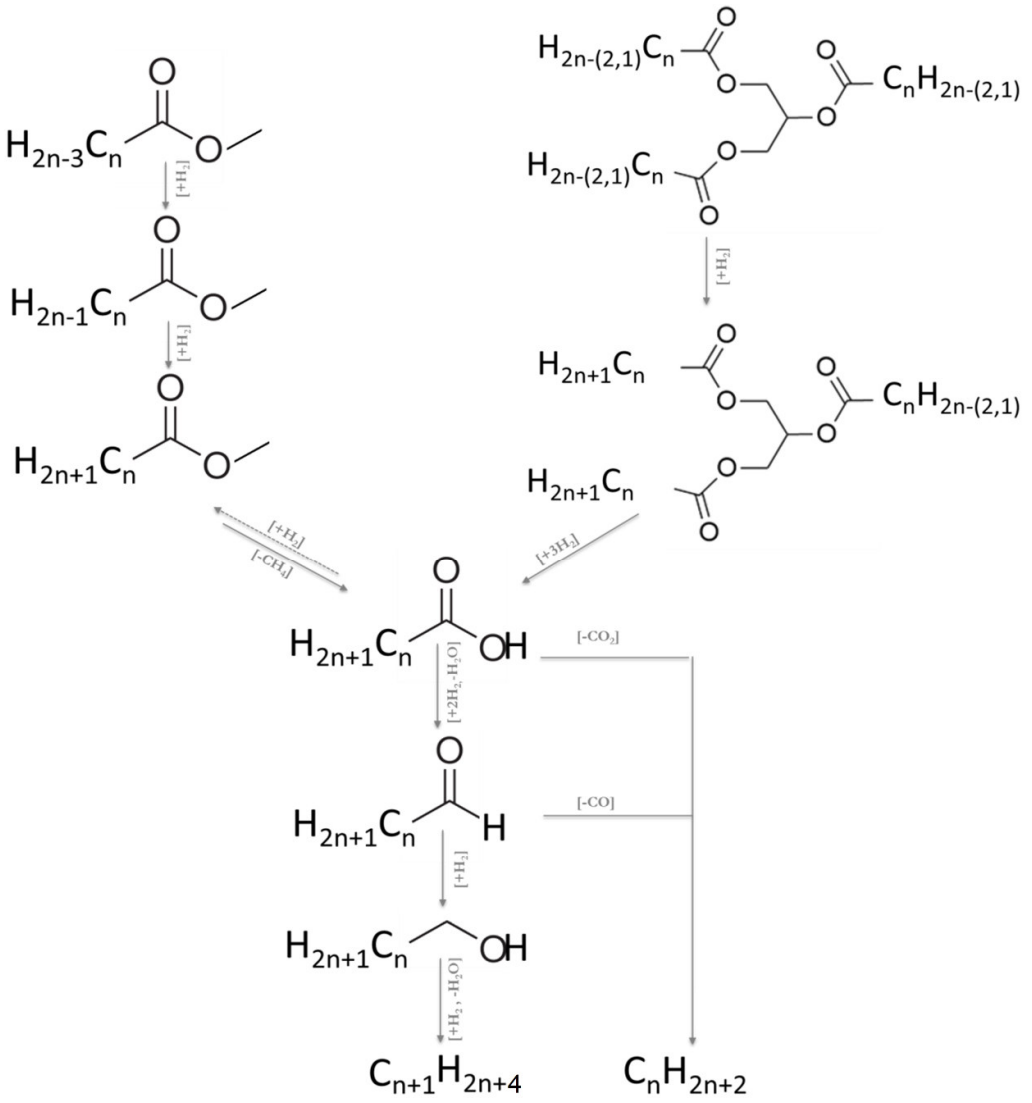

Scheme 1. Reaction pathways for FAME and TG HDO, with n=15 and 17.

The products were aliphatic hydrocarbons with 15-18 carbon number. Considering a number of carbons per molecule, all reactions can be divided into two groups: C:18 HDO and C:16 HDO.

The mechanism of HDO of fatty acids in the presence of heterogeneous catalysts is rather well established [10,16,28].

Molecules with a slightly different carbon chain length, C:16 and C:18, show similar behavior. Therefore, the same type of reaction network can be used for both reactions.

The network for C18 and C16 esters (respectively MLE and MPE) as well as triglycerides (TG) is sketched in **Scheme 2**.

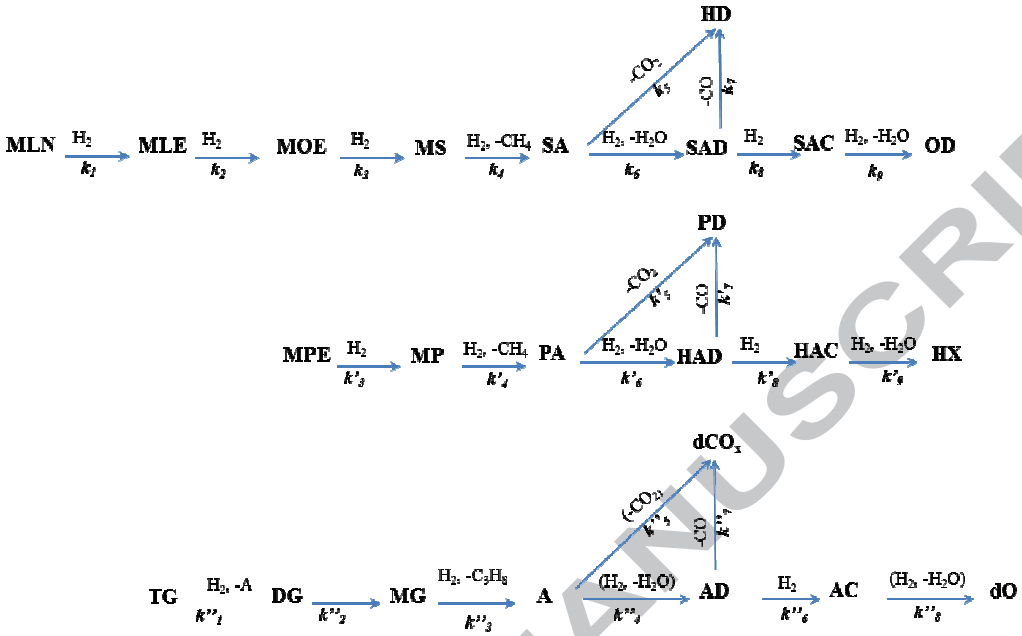

Scheme 2. Reaction network.

For C18 substrate the reaction mechanism consist of 9 reactions and can be written as:

$$MLN + H_2 \longrightarrow MLE \quad (1)$$

$$MLE + H_2 \longrightarrow MOE \quad (2)$$

$$MOE + H_2 \longrightarrow MS \quad (3)$$

$$MS + H_2 \longrightarrow SA + CH_4 \quad (4)$$

$$SA \longrightarrow HD + CO_2 \quad (5)$$

$$SA + H_2 \longrightarrow SAD + H_2O \quad (6)$$

$$SAD \longrightarrow HD + CO \quad (7)$$

$$SAD + H_2 \longrightarrow SAC \quad (8)$$

$$SAC + H_2 \longrightarrow OD + H_2O \quad (9)$$

Eqns. 1-3 represent hydrogenation of unsaturated methyl esters (methyl linolenate methyl (MLN), linoleate (MLE), methyl oleate (MOE)) followed by conversion of methyl stearate (MS) into stearic acid (SA) by a hydrogenolysis reaction releasing methane (eq. 4). Eq. 5 represents decarboxylation of SA into heptadecane (HD). Eq. 6 displays hydrogenation-dehydration of SA into stearyl aldehyde (SAD). Hydrogenation of SAD in eq. 8 leads to formation of stearyl alcohol (SAC) which follows thereafter a dehydration-hydrogenation reaction leading to formation of octadecane (OD) as shown in eq. 9. Moreover, SAD follows also a decarbonylation reaction (eq. 7) to generate HD. Reactions 5 and 7 indicate respectively decarboxylation and decarbonylation reactions.

Mass balance for a particular compound in a batch reactor with the constant volume is:

$$\frac{dC_i}{dt} = R_i \tag{10}$$

where $R_i = \sum \upsilon_i r_i$ (11)

The generation rates of the compounds are obtained from the stoichiometric coefficients ν_{ij} of component i in reaction j. For the present system it can be written

$$R_{MLN} = -r_1 \tag{12}$$

$$R_{MLE} = r_1 - r_2 \tag{13}$$

$$R_{MOE} = r_2 - r_3 \tag{14}$$

$$R_{MS} = r_3 - r_4 \tag{15}$$

$$R_{SA} = r_4 - r_5 - r_6 = 0 \tag{16}$$

$$R_{SAD} = r_6 - r_7 - r_8 = 0 \tag{17}$$

$$R_{SAC} = r_8 - r_9 = 0 \tag{18}$$

$$R_{HD} = r_5 + r_7 \quad (19)$$

$$R_{OD} = r_9 \quad (20)$$

In the denominator of rate equations only the adsorption constant K_A for acids was included in the expressions for reaction rates exempting other functional groups (aldehydes, esters, alcohol and hydrocarbons) as typically much less strongly adsorbed. In practice as the concentration of linoleic and oleic acids in the case of methyl linoleate HDO is low, only concentration of stearic acid was considered.

By lumping catalyst concentration and adsorption constants of reactants into the corresponding rate constants in k_i (i=1-9), and incorporating hydrogen pressure dependence in the rate constants only for steps involving hydrogen (e.g. k_i with i=1-4,6,8,9), the generation equations for components become

$$\frac{dc_{MLN}}{dt} = \frac{-k_1\, c_{MLN}}{(1+K_A c_{SA})} \quad (20)$$

$$\frac{dc_{MLE}}{dt} = \frac{k_1\, c_{MLN} - k_2\, c_{MLE}}{(1+K_A c_{SA})} \quad (21)$$

$$\frac{dc_{MOE}}{dt} = \frac{k_2\, c_{MLE} - k_3\, c_{MOE}}{(1+K_A c_{SA})} \quad (22)$$

$$\frac{dc_{MS}}{dt} = \frac{k_3\, c_{MOE} - k_4\, c_{MS}}{(1+K_A c_{SA})} \quad (23)$$

$$\frac{dc_{SA}}{dt} = \frac{k_4\, c_{MS} - k_5\, c_{SA} - k_6\, c_{SA}}{(1+K_A c_{SA})} \quad (24)$$

$$\frac{dc_{SAD}}{dt} = \frac{k_6\, c_{SA} - k_7\, c_{SAD} - k_8\, c_{SAD}}{(1+K_A c_{SA})} \quad (25)$$

$$\frac{dc_{SAC}}{dt} = \frac{k_8\, c_{SAD} - k_9\, c_{SAC}}{(1+K_A c_{SA})} \quad (26)$$

$$\frac{dc_{HD}}{dt} = \frac{k_5\, c_{SA} + k_7\, c_{SAD}}{(1+K_A c_{SA})} \quad (27)$$

$$\frac{dc_{OD}}{dt} = \frac{k_9\, c_{SAC}}{(1+K_A c_{SA})} \quad (28)$$

The system consisting of equations 20-28 represent the mathematical model of the FAME HDO kinetics.

The system of differential equations (eqns. 20-28) was solved numerically using the backward difference method. The problem was solved by system optimization through calculating factors conditioned by minimizing the deviation from experimental concentrations. The code was written in Fortran programing language. The calculated constants for all reactions are summarized in Table 1.

Table 1. Estimated parameters for fatty acids methyl esters

5 wt% Ni/H-Y-80							
	16 carbon				18 carbon		
Parameters	Estimated value	Unit	*Residual standard error RSS (%)*	Parameters	Estimated value	Unit	*Residual standard error RSS (%)*
—	—	—	—	k_1	5.15×10^{-1}	min^{-1}	0.03
—	—	—	—	k_2	7.41×10^{-1}	min^{-1}	0.06
k'_3	3.00×10^{-1}	min^{-1}	9.7	k_3	8.05×10^{-1}	min^{-1}	$<10^{-5}$
k'_4	5.01×10^{-2}	min^{-1}	8.7	k_4	1.09×10^{-2}	min^{-1}	3.38
k'_5	5.00×10^{-3}	min^{-1}	$<10^{-5}$	k_5	1.00×10^{-2}	min^{-1}	$<10^{-5}$
k'_6	4.25×10^{-2}	min^{-1}	1.47	k_6	7.50×10^{-2}	min^{-1}	2.75
k'_7	1.14×10^{0}	min^{-1}	7.95	k_7	2.09×10^{0}	min^{-1}	7.94
k'_8	$1.00 \times 10^{+1}$	min^{-1}	0.04	k_8	$1.70 \times 10^{+1}$	min^{-1}	0.63
k'_9	6.02×10^{-1}	min^{-1}	1.13	k_9	7.71×10^{-1}	min^{-1}	4.05
K'_A	1.01×10^{-2}	$L\ mol^{-1}$	—	K_A	1.13×10^{-2}	$L\ mol^{-1}$	—
5 wt% Pd/C							
	16 carbon				18 carbon		
Parameters	Estimated value	Unit	*Relative standard error (%)*	Parameters	Estimated value	Unit	*Relative standard error (%)*
—	—	—	—	k_1	3.65×10^{-1}	min^{-1}	8.65
—	—	—	—	k_2	4.25×10^{-1}	min^{-1}	0.89
k'_3	2.50×10^{-1}	min^{-1}	2.35	k_3	6.19×10^{-1}	min^{-1}	$< 10^{-5}$
k'_4	1.63×10^{-3}	min^{-1}	3.71	k_4	2.01×10^{-3}	min^{-1}	6.5
k'_5	1.00×10^{-3}	min^{-1}	1.97	k_5	1.90×10^{-3}	min^{-1}	2.97
k'_6	1.33×10^{-4}	min^{-1}	$< 10^{-5}$	k_6	2.53×10^{-4}	min^{-1}	$< 10^{-5}$
k'_7	1.22×10^{-1}	min^{-1}	2.42	k_7	8.85×10^{-1}	min^{-1}	1.09
k'_8	7.99×10^{0}	min^{-1}	1.19	k_8	1.18×10^{1}	min^{-1}	2.41
k_9	1.82×10^{-3}	min^{-1}	0.22	k_9	7.44×10^{-2}	min^{-1}	4.17
K'_A	1.01×10^{-2}	$L\ min^{-1}$	~	K_A	1.10×10^{-2}	$L\ min^{-1}$	~

The residual sum of squares (R) was calculated using the method of the least squares:

$$R^2 = \sum_i \sum_t \left(C_{it(\exp)} - C_{it(model)}\right)^2 \quad (27)$$

Where the subscripts *i* and *t* refer to components and the time respectively.

The estimation results show a relatively good agreement between the experimentally obtained and predicted concentrations. The residual standard errors for the most of estimated concentration profiles are within few percent. The overall degree of explanation was 99.67% for C:18 and 99.93% for C:16 substrates in the case of Ni catalyst and 99.54% for C:18 and 99.40% for C:16 substrates in the case of Pd.

The values of constants k_7, k_8, k'_7, k'_8 are in agreement with the high rate of aldehydes transformation. The values of constants k_6, k'_6 are approximately 8 fold k_5, k'_5 in case of Ni leading to faster transformations of acids into aldehydes than to hydrocarbons by decarboxylation route. Moreover, k_8, k'_8 are higher than k_7, k'_7, indicating that the deoxygenation pathway (following reactions 8, 9) was the most prominent. In the case of Pd, k_5, k'_5 are 7.5 folds k_6, k'_6 which is in agreement with the numerous studies [13, 29–32] showing that FA HDO over palladium follows decarboxylation/decarbonylation pathways.

Calculated values k'_i, k_i reveal that the rate constants are dependent on the molecule chain length. Reddy and Sunil [24] reported that the rate constants for conversion of FA are independent the fatty acid chain length in their study of TG HDO conversion over an alumina supported nickel catalyst. It was claimed that the rate constants for palmitic acid and stearic acid transformation into alkanes are closely matching each other. However, in our study, there were clear differences in the values of constants. This was noticed for both Ni and Pd catalysts.

An overall decrease in the rate constants was seen for Pd in comparison with Ni. For hydrogenation steps, the constants are in the same range for both catalysts, however when methyl stearate and methyl palmitate are transformed respectively into stearic and

palmitic acids, their corresponding constants k_4, k'_4 decrease by two orders of magnitude. This is noticed also for $k_{5\text{-}6}$, $k'_{5\text{-}6}$ corresponding to acids transformation into alkanes and aldehydes.

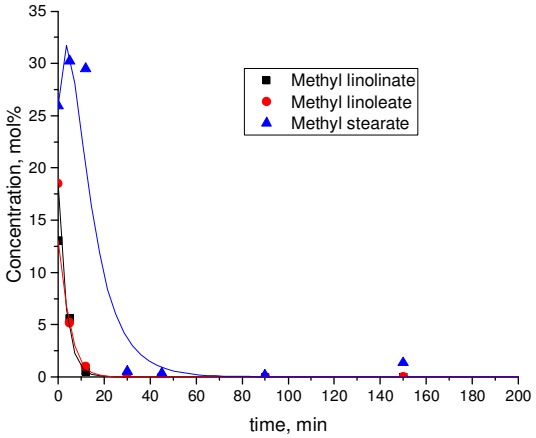

a)

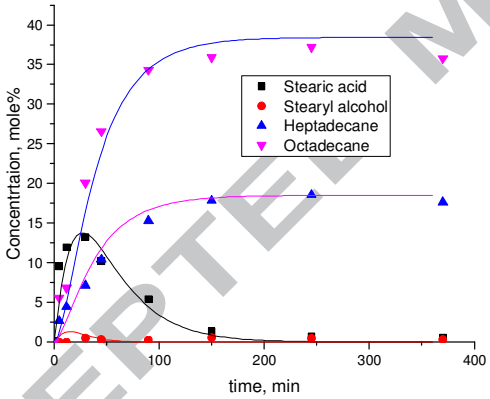

b)

Figure 1. Model fit to the experimental data of FAME HDO over 5wt % Ni/H-Y-80. a) reactants, b) intermediates and hydrocarbons for 18 carbon chain group. Experimental points- symbols, calculations- lines.

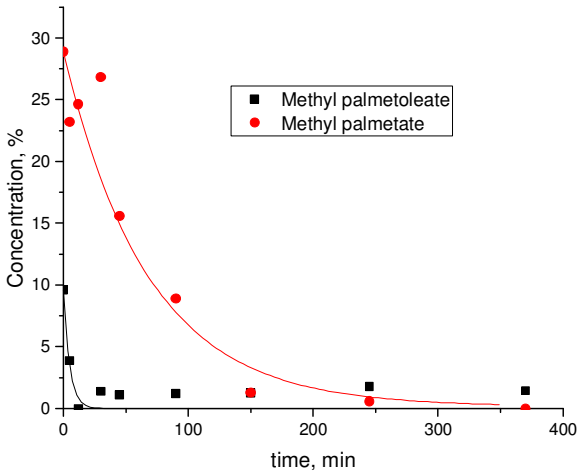

a)

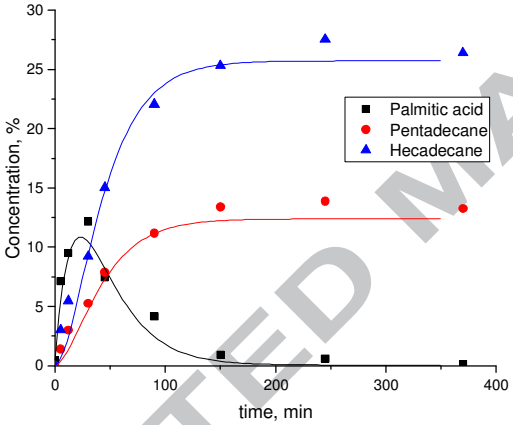

b)

Figure 2. Model fit to the experimental data of FAME HDO over 5 wt % Ni/H-Y-80: a) reactants, b) intermediates and hydrocarbons for 16 carbon chain group. Experimental points- symbols, calculations- lines.

Figures 1-4 display how the model predicts the concentration profiles of the reactants, intermediates and products as a function of time in the reaction performed at 300 °C and pressure 30 bar over Ni/H-Y zeolites (**Figures 1, 2**) and Pd/C (**Figures 3, 4**). While the calculations were done using the mole concentrations, for better visualization the mole fractions are presented in Figure 1-4.

The model takes into account the initial increase of methyl stearate concentration (**Figure 1-a)** due to hydrogenation of methyl esters of unsaturated fatty acids over Ni catalyst. Similarly, the same behavior is observed for methyl stearate concentration in **Figures 3** when Pd catalyst was used**.** Thereafter there was a fast decrease of methyl stearate concentration due to its further transformation into stearic acid. In a similar way palmitic acid is formed from transformations of methyl palmitate and methyl palmitoleate (**Figures 2-a, 4**). As a consequence, unsaturated esters hydrogenation follows a similar path irrespective of the catalyst used.

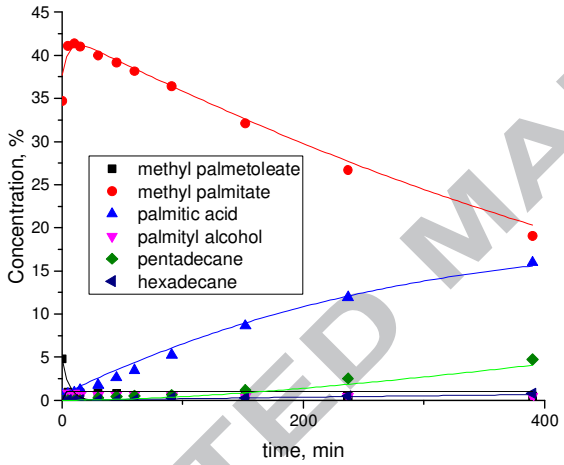

Figure 3. Model fit to the experimental data of FAME HDO over 5 wt. % Pd/C. Experimental points- symbols, calculations- lines.

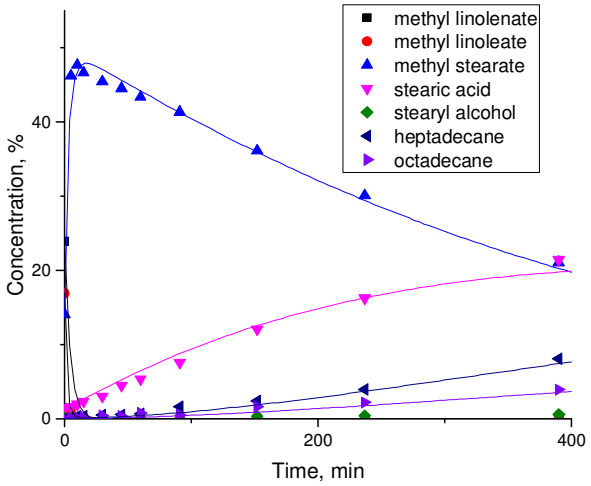

Figure 4. Model fit to the experimental data of FAME HDO over 5 wt. % Pd/C. Experimental points- symbols, calculations- lines.

The profiles of intermediates and products, namely acids, alcohols and hydrocarbons are displayed in **Figures 1-b, 2-b** for FAME HDO over Ni and **Figures 3, 4** for FAME HDO over Pd. Ni showed a higher selectivity towards hydrodeoxygenation products while Pd was more selective to decarboxylation/decarbonylation products. This is also reflected in the absolute values of the corresponding rate constants.

During the parameter estimation, some calculations were done neglecting the adsorption constant of the acid. It turned out that this simplification resulted in systematic deviations of the calculated concentrations from the experimental data. Therefore, it was important to include the adsorption coefficients in the model, such as for example done in kinetic modelling of methyl palmitate HDO over a bifunctional Rh/ZrO_2 catalyst [25,33].

Excellent correspondence of the fit to the data confirms that the reaction network was adequately described not requiring inclusion of any additional parameters.

In the case of triglycerides HDO, the modeling results also concur well with the experimental data with the correlation coefficient 99.99%.

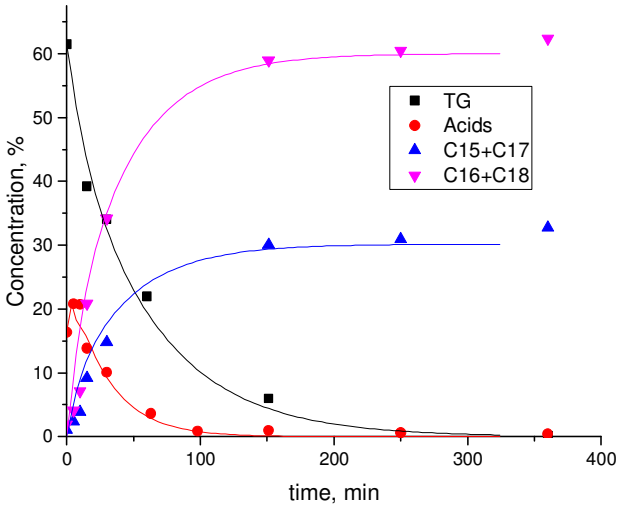

Figure 5. Model fit to the experimental molar animal fat TG conversion profile as a function of time over a Ni catalyst. Experimental points- symbols, calculations- lines.

As illustrated in **Figure 5**, the model predicts correctly the kinetic behavior of animal fat TG HDO with a minor deviation for the acid. The values of calculated and estimated rate constants and the relative standard errors for conversion of triglycerides are displayed in Table 2. Due to the complexity of the mixture the different molecules were regrouped based on their function instead of their molecular length.

The values of k8, k'8 and k''6 given in Tables 1 and 2 are the optimized values obtained by numerical data fitting. Lower values would influence the quality of the overall fit by displaying larger deviations of the calculated concentrations leading to their larger deviations from the experimental observations.

Table 2. Estimated parameters for triglycerides HDO over Ni catalyst.

Parameters	Estimated value[min^{-1}]	Unit	*Residual standard error RSS (%)*
k''_1	5.12×10^{-1}	min^{-1}	18.24
k''_2	7.41×10^{-1}	min^{-1}	5.99
k''_3	1.09×10^{-1}	min^{-1}	0
k''_4	7.50×10^{-2}	min^{-1}	16.49
k''_5	1.00×10^{-2}	min^{-1}	$<10^{-5}$

k''_6	$1.95 \times 10^{+1}$	min^{-1}	0.19
k''_7	1.82×10^{0}	min^{-1}	10.96
k''_8	4.50×10^{-1}	min^{-1}	5.98
K''_A	1.5×10^{-2}	L mol^{-1}	—

In the work of Reddy and Sunil [24] in kinetic modelling of triglycerides HDO no adsorption terms for any of the compounds were taken into account, being probably the reason for deviations seen at lower temperatures. At the same time the model based on the Eley-Rideal mechanism neglecting adsorption of the acid was reported to be equally good as the Langmuir-Hinshelwood model which includes such adsorption in the case of palmitic acid HDO over Pt/γ-Al_2O_3 [34].

5. Conclusions

Kinetic modelling of fatty acid methyl esters and triglycerides batch-wise hydrodeoxygenation over 5 wt% Ni/H-Y-80 and 5 wt % Pd/C at 300 °C and 30 bar in H_2 was performed. A quantitative analysis of the reaction revealed that substrates in the reaction mixtures can be subdivided into two reacting groups following the same mechanism simplifying treatment of the data. A model based on the reaction mechanism was advanced taking into account adsorption of the reactant and intermediates bearing an acid functional group. The kinetic parameters estimated numerically were well defined allowing obtaining a kinetic model which demonstrated a good fitting to the experimental data. The fatty acid esters with different chain length exhibited different rate constants.

The model accounts for the observed kinetics and explains the concentration dependence of the substrates, intermediates and products successfully. The model is a generic one and can be applied to hydrodeoxygenation of different fatty acids allowing also preliminary reactor sizing and flow sheeting.

Acknowledgment

This work is part of the activities at Johan Gadolin Process Chemistry Centre (PCC) appointed by Åbo Akademi University. The authors are grateful to Dr. Päivi Mäki-Arvela, Dr. Narendra Kumar, Dr. Kari Eränen and Ms. Klara Jeništová for their contribution to the experimental work.

Notation

A= acids
AC= alcohols
AD= aldehydes
C = concentration
dCO_x= decarboxylation/decarbonylation products
DG= diglycerides
dO= deoxygenation products
HAC = 1-hexadecanol
HD = heptadecane
HX = hexadecane
k= rate constant
K_A= acid constant
MD= monoglycerides
MLE = methyl linoleate
MLN = methyl linolenate
MOE = methyl oleate
MP = methyl palmitate
MPE = methyl palmitoleate
MS = methyl stearate
OD= octadecane
PA = palmitic acid
PAD = palmitoyl aldehyde (1-hexadecanal)
PD = pentadecane
SAD = stearyl aldehyde
r = partial rate
R_i = rate of component i
SA = stearic acid
SAC = stearyl alcohol
t = time
TG= triglycerides

Subscripts

1-9 = reaction step number
i = component i
j = reaction step number

Fortran PowerStation version 4.00.5277
Product ID: 36785-040-0004145-57177

References

[1] European Environment Agency, Greenhouse gas emission trends and projections in Europe 2012, Denmark, 2012. doi:10.2800/56770.

[2] S. Boonyasuwat, J. Tscheikuna, Co-processing of palm fatty acid distillate and light gas oil in pilot-scale hydrodesulfurization unit over commercial CoMo / Al_2O_3, Fuel. 199 (2017) 115–124.

[3] K. Kon, T. Toyao, W. Onodera, S.M.A.H. Siddiki, K. Shimizu, Hydrodeoxygenation of fatty acids, triglycerides, and ketones to liquid alkanes by a Pt–MoO_x/TiO_2 Catalyst, ChemCatChem. 9 (2017) 2822–2827.

[4] M. Snåre, I. Kubickova, P. Mäki-Arvela, K. Eränen, D.Yu.Murzin, Heterogeneous catalytic deoxygenation of stearic acid for production of biodiesel, Ind. Eng. Chem. Res., 45 (2006) 5708-5715.

[5] C. Kordulis, K. Bourikas, M. Gousi, E. Kordouli, A. Lycourghiotis, Development of nickel based catalysts for the transformation of natural triglycerides and related compounds into green diesel : a critical review, Appl. Catal. B : Environ. 181 (2016) 156–196.

[6] V.K. Soni, P.R. Sharma, G. Choudhary, S. Pandey, R.K. Sharma, Ni/Co-natural clay as green catalysts for microalgae oil to diesel- grade hydrocarbons conversion, ACS Sustain. Chem. Eng. 5 (2017) 5351–5359.

[7] J. Wu, J. Shi, J. Fu, J.A. Leidl, Z. Hou, X. Lu, Catalytic decarboxylation of fatty acids to aviation fuels over nickel supported on activated carbon, Sci. Rep. 6 (2016)..

[8] E. Santillan-Jimenez, T. Morgan, J. Shoup, A.E. Harman-Ware, M. Crocker, Catalytic deoxygenation of triglycerides and fatty acids to hydrocarbons over Ni–Al layered double hydroxide, Catal. Today. 237 (2014) 136–144..

[9] O.I. Şenol, E.M. Ryymin, T.-R. Viljava, A.O.I. Krause, Effect of hydrogen sulphide on the hydrodeoxygenation of aromatic and aliphatic oxygenates on sulphided catalysts, J. Mol. Catal. A Chem. 277 (2007) 107–112..

[10] B. Peng, C. Zhao, S. Kasakov, S. Foraita, J.A. Lercher, Manipulating catalytic pathways: Deoxygenation of palmitic acid on multifunctional catalysts, Chem. - A Eur. J. 19 (2013) 4732–4741.

[11] I. V Deliy, E.N. Vlasova, A.L. Nuzhdin, G.A. Bukhtiyarova, The comparison of sulfide CoMo/γ-Al_2O_3 and NiMo/γ-Al_2O_3 catalysts in methyl palmitate and methyl heptanoate hydrodeoxygenation, Recent Res. Eng. Autom. Control. (2011) 24–29.

[12] B. Peng, X. Yuan, C. Zhao, J.A. Lercher, Stabilizing catalytic pathways via redundancy: selective reduction of microalgae oil to alkanes, J. Am. Chem. Soc. 134 (2012) 9400–9405.

[13] A.A. Stepacheva, L.Z. Nikoshvili, E.M. Sulman, V.G. Matveeva, Hydrodeoxygenation of stearic acid for the production of green diesel, Green Process. Synth. 3 (2014) 441–446.

[14] B. Donnis, R.G. Egeberg, P. Blom, K.G. Knudsen, Hydroprocessing of bio-oils and oxygenates to hydrocarbons. Understanding the reaction routes, Top. Catal. 52 (2009) 229–240.

[15] P. Šimáček, D. Kubička, G. Šebor, M. Pospíšil, Hydroprocessed rapeseed oil as a source of hydrocarbon-based biodiesel, Fuel. 88 (2009) 456–460.

[16] I. Hachemi, N. Kumar, P. Mäki-Arvela, J. Roine, M. Peurla, J. Hemming, J. Salonen, D. Yu. Murzin, Sulfur-free Ni catalyst for production of green diesel by hydrodeoxygenation, J. Catal. 347 (2017) 205–221.

[17] H. Zuo, Q. Liu, T. Wang, L. Ma, Q. Zhang, Q. Zhang, Hydrodeoxygenation of methyl palmitate over supported ni catalysts for diesel-like fuel production, Energy and Fuels. 26 (2012) 3747–3755.

[18] K. Jeništová, I. Hachemi, P. Mäki-Arvela, N. Kumar, M. Peurla, L. Čapek, J. Wärnå, D.Y. Murzin, Hydrodeoxygenation of stearic acid and tall oil fatty acids over Ni-alumina catalysts : Influence of reaction parameters and kinetic modelling, Chem. Eng. J. 316 (2017) 401–409.

[19] W. Song, C. Zhao, J.A. Lercher, Importance of size and distribution of Ni nanoparticles for the hydrodeoxygenation of microalgae oil, Chem. - A Eur. J. 19 (2013) 9833–9842.

[20] R.W. Gosselink, S.A.W. Hollak, S.-W. Chang, J. Van Haveren, K.P. De Jong, J.H. Bitter, D.S. van Es, Reaction pathways for the deoxygenation of vegetable oils and related model compounds, ChemSusChem. 6 (2013) 1576–1594.

[21] C.V. Viêgas, I. Hachemi, S.P. Freitas, P. Mäki-Arvela, A. Aho, J. Hemming, A. Smeds, I. Heinmaa, F.B. Fontes, D.C. da Silva Pereira, N. Kumar, D.A.G.

Aranda, D.Yu. Murzin, A route to produce renewable diesel from algae: Synthesis and characterization of biodiesel via in situ transesterification of Chlorella alga and its catalytic deoxygenation to renewable diesel, Fuel. 155 (2015) 144–154.

[22] V. Kuuluvainen, P. Maki-Arvela, A.-R. Rautio, K. Kordás, J. Roine, A. Aho, B. Toukoniitty, Blanka, H. Österholm, M. Toivakka, D.Y. Murzin, Properties of adsorbents used for bleaching of vegetable oils and animal fats, J. Chem. Technol. Biotechnol. 90 (2015) 1579–1591.

[23] B. Rozmysłowicz, A. Kirilin, A. Aho, H. Manyar, C. Hardacre, J. Wärnå, T. Salmi, D. Yu. Murzin, Selective hydrogenation of fatty acids to alcohols over highly dispersed ReO x / TiO_2 catalyst, J. Catal. 328 (2015) 197–207.

[24] S. Reddy, Y. Sunil, Reaction mechanism and kinetic modeling for the hydrodeoxygenation of triglycerides over alumina supported nickel catalyst, React. Kinet. Mech. Catal. 120 (2017) 109–128.

[25] Y. Bie, J. Lehtonen, J. Kanervo, Hydrodeoxygenation (HDO) of methyl palmitate over bifunctional Rh/ZrO_2 catalyst : Insights into reaction mechanism via kinetic modeling, Applied Catal. A. Gen. 526 (2016) 183–190.

[26] I. Hachemi, K. Jeništová, P. Mäki-Arvela, N. Kumar, K. Eränen, J. Hemming, D.Y. Murzin, Comparative study of sulfur-free nickel and palladium catalysts in hydrodeoxygenation of different fatty acid feedstocks for production of biofuels, Catal. Sci. Technol. 6 (2016) 1476–1487.

[27] V. Kuuluvainen, P. Mäki-Arvela, K. Eränen, A. Holappa, J. Hemming, H. Österholm, B. Toukoniitty, D.Yu. Murzin, Extraction of spent bleaching earth in the production of renewable diesel, Chem. Eng. Technol. 38 (2015) 769–776.

[28] K. Kandel, J.W. Anderegg, N.C. Nelson, U. Chaudhary, I.I. Slowing, Supported iron nanoparticles for the hydrodeoxygenation of microalgal oil to green diesel, J. Catal. 314 (2014) 142–148.

[29] J.G. Immer, M.J. Kelly, H.H. Lamb, Catalytic reaction pathways in liquid-phase deoxygenation of C18 free fatty acids, Appl. Catal. A Gen. 375 (2010) 134–139.

[30] A. Theilgaard Madsen, B. Rozmyslowicz, I. Simakova, T. Kilpiö, A.-R. Leino, K. Kordas, K. Eränen, P. Mäki-Arvela, D.Yu. Murzin, Step changes and deactivation behavior in the continuous decarboxylation of stearic acid, Ind. Eng. Chem. Res., 50 (2011) 11049-11058.

[31] I. Simakova, O. Simakova, P. Mäki-Arvela, A. Simakov, M. Estrada, D.Yu. Murzin, Deoxygenation of palmitic and stearic acid over supported Pd catalysts: effect of metal dispersion, Appl. Catal. A. General, 355 (2009) 100-108.

[32] T.-W. Kim, S.-R. Hwang, Y.-W, Suh, C,-U. Kim, Deoxygenation of fatty acid over three-dimensionally ordered mesoporous carbon supported palladium catalysts, Top. Catal. 60 (2017) 677–684.

[33] Y. Bie, J.M. Kanervo, J. Lehtonen, Hydrodeoxygenation of methyl heptanoate over Rh/ZrO_2 catalyst as a model reaction for biofuel production : Kinetic modeling based on reaction mechanism, Ind. Eng. Chem. Res. 48 (2015) 11986–11996.

[34] L. Zhou, A. Lawal, Kinetic study of hydrodeoxygenation of palmitic acid as a model compound for microalgae oil over Pt /γ-Al_2O_3, Appl. Catal. A. Gen. 532 (2017) 40–49.

- Kinetics of fatty acids methyl esters and triglycerides hydrodeoxygenation
- Pd/C and sulfur free 5wt % Ni/H-Y-80 catalysts
- Reaction network involves hydrogenation, deoxygenation and direct hydrodeoxygenation
- Adequate fitting for both studied substrates
- Rate constants show dependence on the fatty acids carbon chain length